Sip2p and its partner Snf1p kinase affect aging in *S. cerevisiae*

Kaveh Ashrafi, Stephen S. Lin, Jill K. Manchester, and Jeffrey I. Gordon[1]

Department of Molecular Biology and Pharmacology, Washington University School of Medicine, St. Louis, Missouri 63110 USA

For a number of organisms, the ability to withstand periods of nutrient deprivation correlates directly with lifespan. However, the underlying molecular mechanisms are poorly understood. We show that deletion of the N-myristoylprotein, Sip2p, reduces resistance to nutrient deprivation and shortens lifespan in *Saccharomyces cerevisiae*. This reduced lifespan is due to accelerated aging, as defined by loss of silencing from telomeres and mating loci, nucleolar fragmentation, and accumulation of extrachromosomal rDNA. Genetic studies indicate that *sip2Δ* produces its effect on aging by increasing the activity of Snf1p, a serine/threonine kinase involved in regulating global cellular responses to glucose starvation. Biochemical analyses reveal that as yeast age, hexokinase activity increases as does cellular ATP and NAD^+ content. The change in glucose metabolism represents a new correlate of aging in yeast and occurs to a greater degree, and at earlier generational ages in *sip2Δ* cells. Sip2p and Snf1p provide new molecular links between the regulation of cellular energy utilization and aging.

[*Key Words*: Aging; *Saccharomyces cervisiae*; N-myristoylproteins; Snf1p kinase interacting protein-2; glucose metabolism; cellular energy storage]

Received April 26, 2000; revised version accepted June 9, 2000.

A direct correlation between lifespan and stress resistance, including resistance to the stress of nutrient deprivation, has been observed in organisms as diverse as *Saccharomyces cerevisiae*, *Caenorhabditis elegans*, and *Drosophila melanogaster* (Service et al. 1985; Arking et al. 1991; Graves et al. 1992; Larsen 1993; Kennedy et al. 1995; Lithgow et al. 1995). Similarly, mice raised on a calorically restricted diet have extended maximal lifespans and exhibit a delay in the evolution of aging-associated physiologic and pathologic changes (Arking 1998; Lee et al. 1999). Although the correlation between stress resistance and lifespan has been used to identify several genes that affect longevity, it remains poorly understood at a molecular level (Kenyon et al. 1993; Orr and Sohal 1994; Kennedy et al. 1995; Morris et al. 1996; Murakami and Johnson 1996; Ewbank et al. 1997; Kimura et al. 1997; Lin et al. 1997, 1998).

A recent analysis of the expression patterns of 6347 genes in the mouse gastrocnemius muscle indicated that aging is associated with a significant (≥~2-fold) increase or decrease in the steady state levels of 113 mRNAs (Lee et al. 1999). Of the 58 mRNAs that increase with age, 16% encode proteins involved in stress responses (e.g., oxidative damage and heat shock). Of the 55 mRNAs that decrease with age, 13% encode enzymes involved in various aspects of energy metabolism. Compared to age-matched controls, calorie-restricted mice manifest reduced expression of genes that participate in stress responses and DNA repair. There is also increased expression of genes that regulate glycolysis (glucose-6-phosphate isomerase) and gluconeogenesis (fructose-1,6-bisphosphatase), and that inhibit glycogen synthesis (IPP-2). These expression profiles indicate that aging is associated with a decline in metabolic activity while chronic caloric restriction produces a shift toward increased energy metabolism and gluconeogenesis.

One of the challenges presented by this type of comprehensive profiling of gene expression is to identify simplified experimental models where genetic and biochemical tests can be performed to decipher how these or other responses to nutrient deprivation regulate and/or mediate the aging process. *S. cerevisiae* provides one such model. Individual yeast cells undergo a limited number of divisions prior to cessation of growth (Mortimer and Johnston 1959). Different strains have characteristic mean and maximum lifespans, indicating an underlying genetic basis for aging (Kennedy et al. 1995). Mutations in the RecQ-like helicase, Sgs1p, have been reported to cause accelerated aging in yeast. Rapid aging is manifested by reduced generational lifespan, sterility, redistribution of the Sir transcriptional silencing complex from *HM* loci and telomeres to the nucleolus, changes in nucleolar morphology, and accumulation of extrachromosomal rDNA circles (ERCs; Sinclair and Guarente 1997; Sinclair et al. 1997). Mutations in the

[1]Corresponding author.
E-MAIL jgordon@molecool.wustl.edu; FAX (314) 362 7047.

human homolog of *SGS1* also affect longevity, producing the premature aging phenotype of Werner's syndrome (Yu et al. 1996).

In rich media, *S. cerevisiae* utilizes glucose as its preferred carbon source. When glucose becomes limiting, cells transition from fermentative growth to respiratory growth on alternative carbon sources. *S. cerevisiae* enters a stationary phase when all nutrient sources are exhausted (Werner-Washburne et al. 1993, 1996). The diauxic transition from fermentative to respiratory growth is accompanied by global changes in gene transcription (DeRisi et al. 1997). Remarkably, DNA array analysis of these changes has disclosed some responses that are similar to those produced by caloric restriction in mice, e.g., the induction of fructose 1,6-bisphosphatase, which redirects glycolysis towards glucose-6-phosphate (Lee et al. 1999).

Because of the correlation between the generational lifespan of yeast, and their ability to withstand the stress of nutrient deprivation (Kennedy et al. 1995), we hypothesized that some of the genes that regulate resistance to starvation during stationary phase may also affect aging. We focused our attention on genes encoding N-myristoylproteins. MyristoylCoA:protein N-myristoyltransferase (Nmt1p; Duronio et al. 1989; Bhatnagar et al. 1998) covalently links myristate to proteins that participate in a number of signal transduction cascades (e.g., kinases and their substrates, phosphatases, and the α subunits of heterotrimeric G proteins). N-myristoylation is cotranslational, appears to be irreversible, and in many cases is critical for biological function (for review, see Boutin 1997; Bhatnagar and Gordon 1997). *NMT1* is an essential gene (Duronio et al. 1989). Previously, we had used a temperature sensitive allele (*nmt1–451D*) encoding an enzyme with reduced affinity for myristoylCoA, to establish that deficits in protein N-myristoylation result in decreased resistance to acute and gradual nutrient deprivation, even at permissive temperatures (24°C; Ashrafi et al. 1998). In this report, we have identified an N-myristoylprotein that provides a functional link between cellular aging in yeast and carbon source utilization.

Results

Deficiencies in protein N-myristoylation are associated with all of the known manifestations of accelerated aging in S. cerevisiae

Micromanipulation assays were used to determine whether *nmt1–451D* has any effect on lifespan. Studies conducted at the permissive temperature of 24°C revealed a mean lifespan that was half that of isogenic wild-type cells (14.5 vs. 27.5 generations; Fig. 1A).

A shortened lifespan can reflect accelerated aging or a reduction in cellular fitness. The ability to distinguish between these two possibilities is important: Short-lived mutants are most likely to arise from genetic alterations that have deleterious effects on cellular viability. Sterility accompanies aging in yeast and has been used to distinguish a shortened lifespan due to accelerated aging from a shortened lifespan due to a general loss of fitness (Sinclair et al. 1997). Sterility arises from a loss of silencing at the *HM* mating loci (Smeal et al. 1996). The loss of silencing appears to be attributable to redistribution of a transcriptional silencing complex, composed in part of Sir2p, Sir3p, and Sir4p, from *HM* loci (and telomeres) to the nucleolus (Smeal et al. 1996; Kennedy et al. 1997; Sinclair et al. 1997). We found that the percentage of *nmt1–451D* cells that are sterile increases progressively towards the end of their reduced lifespan (Fig. 1B). This progressive sterility is similar to the pattern observed during the course of aging of isogenic wild-type cells (Fig. 1C).

As noted earlier, nucleolar enlargement and fragmentation, and the localization of Sir complexes to these nucleolar fragments represent other markers of aging in yeast (Sinclair et al. 1997). *nmt1–451D* cells appear normal during their first few divisions, but by generation 7 (50% of their mean lifespan) ~35% have enlarged and/or fragmented nucleoli containing Sir3p. Sir3p is also absent from telomeres ($n = 2$ experiments) (Fig. 2). The percentage of *nmt1–451D* cells that display nucleolar abnormalities and Sir complex redistribution increases further with increasing cell divisions. These changes are not apparent until later generational time points in the wild-type strain, i.e., between generation 7 and 14 (50% of mean lifespan), the number of *NMT1* cells with nucleolar fragmentation and Sir complex redistribution increases from <1% to 16%–18% (1000 cells scored/time point/experiment; $n = 2$ independent experiments).

Sinclair and Guarente (1997) noted that extrachromosomal rDNA circles (ERCs) accumulate as yeast cells age. The *S. cerevisiae* genome contains ~140 rDNA genes clustered together on chromosome XII as 9.1-kb repeats. Homologous recombination between these repeats results in excision of a single rDNA repeat and generation of ERCs (Clark-Walker and Azad 1980; Larionov et al. 1980). ERCs are able to replicate because each rDNA repeat contains an origin of replication (Larionov et al. 1984). Asymmetric segregation of ERCs to mothers occurs after each division, resulting in their exponential accumulation (Sinclair and Guarente 1997). Sinclair and Guarente (1997) proposed that ERCs may promote cell death by titrating essential transcription factors and enzymes involved in DNA replication and repair.

ERC formation was compared in young and older *NMT1* and *nmt1–451D* cells by probing Southern blots of total cellular DNA with a ^{32}P-labeled rDNA fragment. The results reveal that *nmt1–451D* cells contain higher levels of ERCs. By generation 7, the difference is 5-fold ($n = 3$ experiments; Fig. 3). Thus, *nmt1–451D* cells satisfy all of the known criteria associated with accelerating aging in *S. cerevisiae*.

Loss of Sip2p recapitulates the rapid aging phenotype of nmt1–451D *cells*

Because the enzymatic defects of nmt451Dp can affect levels of N-myristoylation of one or more of its substrates, these results raise the question of which N-my-

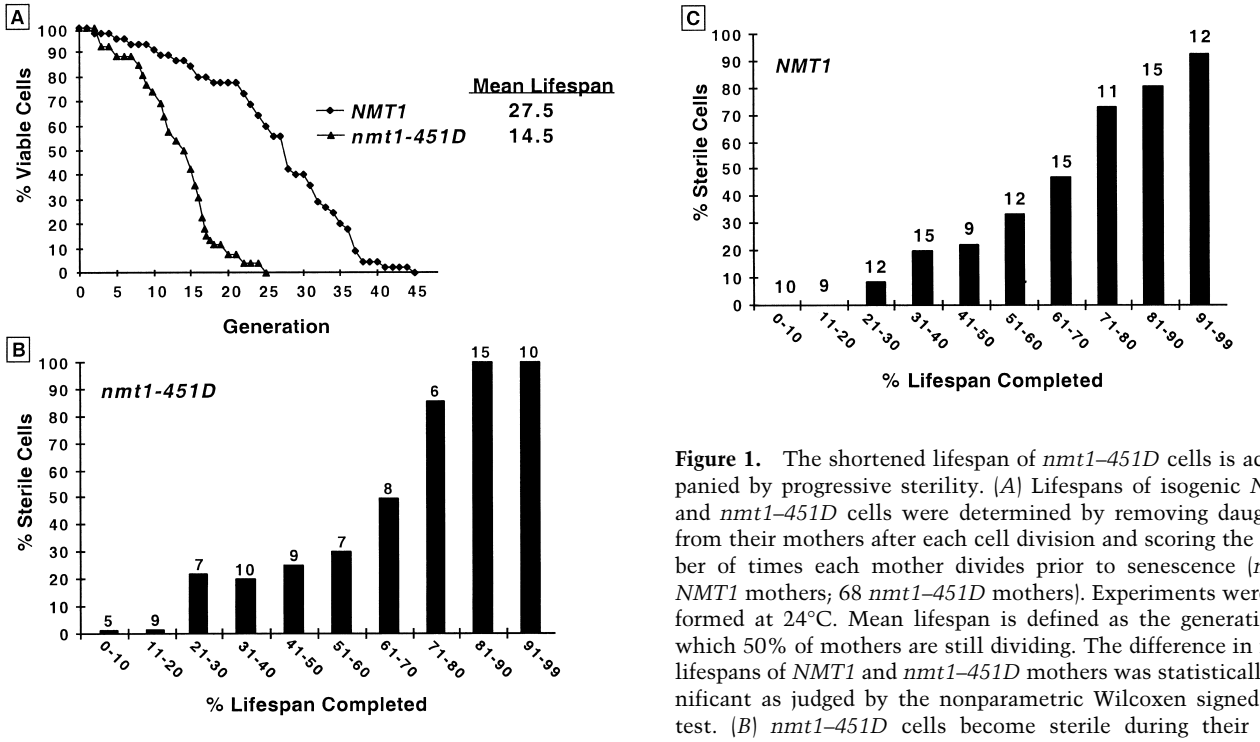

Figure 1. The shortened lifespan of *nmt1–451D* cells is accompanied by progressive sterility. (*A*) Lifespans of isogenic *NMT1* and *nmt1–451D* cells were determined by removing daughters from their mothers after each cell division and scoring the number of times each mother divides prior to senescence ($n = 85$ *NMT1* mothers; 68 *nmt1–451D* mothers). Experiments were performed at 24°C. Mean lifespan is defined as the generation at which 50% of mothers are still dividing. The difference in mean lifespans of *NMT1* and *nmt1–451D* mothers was statistically significant as judged by the nonparametric Wilcoxen signed rank test. (*B*) *nmt1–451D* cells become sterile during their short lifespan. Numbers that appear above each bar represent the number of cells whose pheromone response was scored at this point in their lifespan. At various generation times, individual *MAT***a** cells were moved near to a disk soaked in 0.25 μM α-factor. Four hours later they were scored for shmooing. They were then moved to an area of the YPD/agar plate away from the source of pheromone and allowed to complete their lifespan. *nmt1–451D* cells that have completed <50% of their lifespan are responsive to pheromone (i.e., they are fertile), while cells that have completed over 70% of their shortened lifespan are almost always sterile. (*C*) Parallel assays of sterility in the isogenic wild-type strain yield results equivalent to those obtained with the *nmt1–451D* strain: the percentage of sterile cells increases progressively as a function of the percentage of lifespan completed. Similar results were obtained when the wild-type strain was assayed at 24°C and at 30°C (data not shown).

ristoylproteins are responsible for the rapid aging phenotype.

The yeast genome contains ≥64 open reading frames (ORFs) encoding known or putative Nmt1p substrates (Ashrafi et al. 1998). In many cases, undermyristoylation of a protein results in its functional inactivation (for review, see Bhatnagar and Gordon 1997). In a recent study (Ashrafi et al. 1998), we disrupted each ORF in wild-type cells and found nine N-myristoylproteins whose loss mimicked the starvation-sensitive phenotype of *nmt1–451D* cells (Arf1p, Arf2p, Ptc2p, Sip2p, Van1p, YBL049W, YJR114W, YKR007W, YMR077C) (see http://genome-www.stanford.edu/Saccharomyces/). Sip2p was selected for further analysis because its removal from wild-type cells produces a more complete loss of viability during stationary phase than any of the other eight N-myristoylproteins, and because it has been linked to a signaling pathway that regulates cellular responses to glucose deprivation.

Sip2p (Snf interacting protein-2) is a member of an evolutionarily conserved and homologous group of proteins that includes Sip1p and Gal83p. All bind to Snf1p with high affinity (Jiang and Carlson 1996, 1997). Snf1p is a serine/threonine kinase required for induction of glucose-repressed genes in response to glucose starvation (Celenza and Carlson 1984, 1986; for review, see Hardie et al. 1998). The induced genes encode proteins involved in the use of alternative carbon sources, gluconeogenesis, and respiration (Celenza and Carlson 1986). The Snf1p pathway is also required for resistance to other forms of environmental stress (Alepuz et al. 1997). *snf1Δ* cells exhibit a number of defects during stationary phase including reduced survival (Thompson-Jaeger et al. 1991). Although the precise role of Sip2p in the Snf1p pathway has not been defined, it physically links Snf1p to its activating subunit, Snf4p, and may serve as an adaptor molecule between Snf1p kinase and some of its substrates (Yang et al. 1994). The three components of the Snf1p kinase complex (Snf1p, Snf4p, and its interacting Sip proteins) are homologous to the subunits of AMP-activated protein kinase, a mammalian cellular fuel gauge involved in regulating cellular stress responses (Hardie et al. 1998).

sip2Δ cells grow normally on glucose-, galactose- or raffinose-containing media, exhibit appropriately regulated *SUC2* (invertase) expression, and sporulate properly (Yang et al. 1994). However, the mean lifespan of *NMT1sip2Δ* cells is reduced to 60% of isogenic wild-type cells (average value from five independent experiments). The reduction is accompanied by all known manifestations of accelerated aging. These cells become sterile during their shortened lifespan (Fig. 4A), display nucleo-

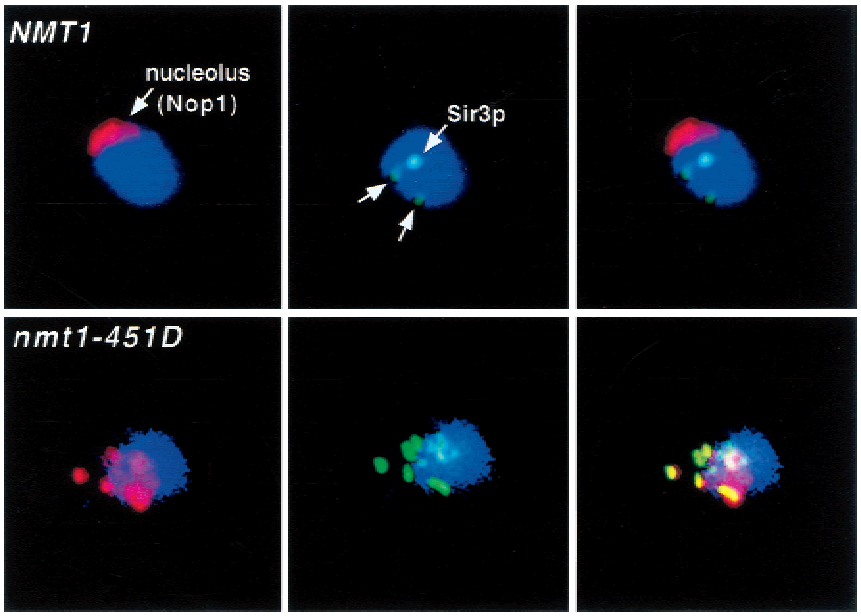

Figure 2. Nucleolar fragmentation and Sir complex redistribution is observed in generation 7 *nmt1–451D* but not *NMT1* cells. Multilabel immunofluorescence study. Fixed *NMT1* cells [average bud scar count (ABSC) = 7.3 ± 3.3] and *nmt1–451D* cells (ABSC = 6.9 ± 2.0) are stained blue with 4′,6′-diamidino-2-phenylindole (DAPI) to visualize nuclear DNA. Nucleoli are marked with antibodies to yeast fibrillarin (Nop1p, red). Sir3p appears green. (*Left* panels) DAPI plus Nop1p; (*middle* panels) DAPI plus Sir3p; (*right* panels) DAPI, Nop1p, and Sir3p. The *NMT1* cell has an intact, crescent-shaped nucleolus and Sir3p appears as telomeric spots. Sir3p is redistributed to a fragmented nucleolus in the *nmt1–451D* cell (colocalization of Sir3p and Nop1p in the nucleolus is seen as yellow).

lar enlargement and fragmentation, and manifest Sir3p redistribution (Fig. 4B). After seven generations, ERC levels in *NMT1sip2Δ* cells are <2-fold greater than age-matched wild-type cells, but by generation 12 they are 10-fold greater (Fig. 4C).

The difference in ERC levels between *NMT1sip2Δ* and *NMT1* cells is less than the difference between *nmt1–451D* and wild-type cells at generation 7, suggesting that in addition to Sip2p, other N-myristoylproteins contribute to the rapid aging phenotype of the *nmt1–451D* strain. However, the mean lifespans of isogenic *nmt1–451D* and *nmt1–451Dsip2Δ* cells are nearly identical (12.5 vs. 14.5 generations, respectively, in a direct comparison; data not shown). This finding supports the notion that Sip2p is the major N-myristoylprotein responsible for the reduced lifespan of *nmt1–451D* cells. Moreover, removal of some of the other candidate N-myristoylproteins from wild-type cells has either no effect on lifespan (e.g., *arf2Δ*, Fig. 5A), or produces a reduction in lifespan but without the concomitant appearance of molecular markers of aging (e.g., *arf1Δ*; Fig. 5A,B).

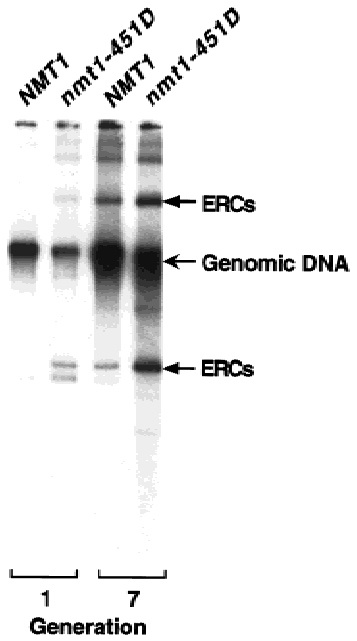

Figure 3. ERC levels are increased in *nmt1–451D* cells. DNA was recovered from *NMT1* cells (ABSC = 0.9 ± 1.1 and 7.2 ± 2.1) and isogenic *nmt1–451D* cells (ABSC = 0.9 ± 1.1 and 6.8 ± 2.6), and fractionated by agarose gel electrophoresis. Southern blots were probed with ^{32}P-labeled rDNA. ERCs and their multimeric derivatives are indicated by arrows.

The reduced lifespan produced by *sip2Δ* is not a unique feature of the genetic background of our S288C-derived wild-type strain (YB332; Table 1). Deletion of *SIP2* in a different wild-type strain (W303) produces a comparable result: The lifespan of YO40 (*sip2Δ*; Table 1) is 71% of its wild-type YO36 parent.

Genetic evidence that sip2Δ *accelerates aging by producing increased or aberrant cellular Snf1p kinase activity*

The effect of Sip2p on aging is not shared by Snf1p's other protein partners. *gal83Δ* has no detectable effect on lifespan, whereas *sip1Δ* reduces lifespan to 82% of wild-type, but without any of the accompanying manifestations of accelerated aging. Therefore, we examined whether the impact of *sip2Δ* on aging was Snf1p-independent or -dependent.

Two observations indicated that diminishing or removing Snf1p activity does not accelerate aging. First, *NMT1snf1Δ* cells have a reduced lifespan (79% of wild-type), but this reduction is not associated with sterility or Sir3p redistribution. Moreover, ERC accumulation is

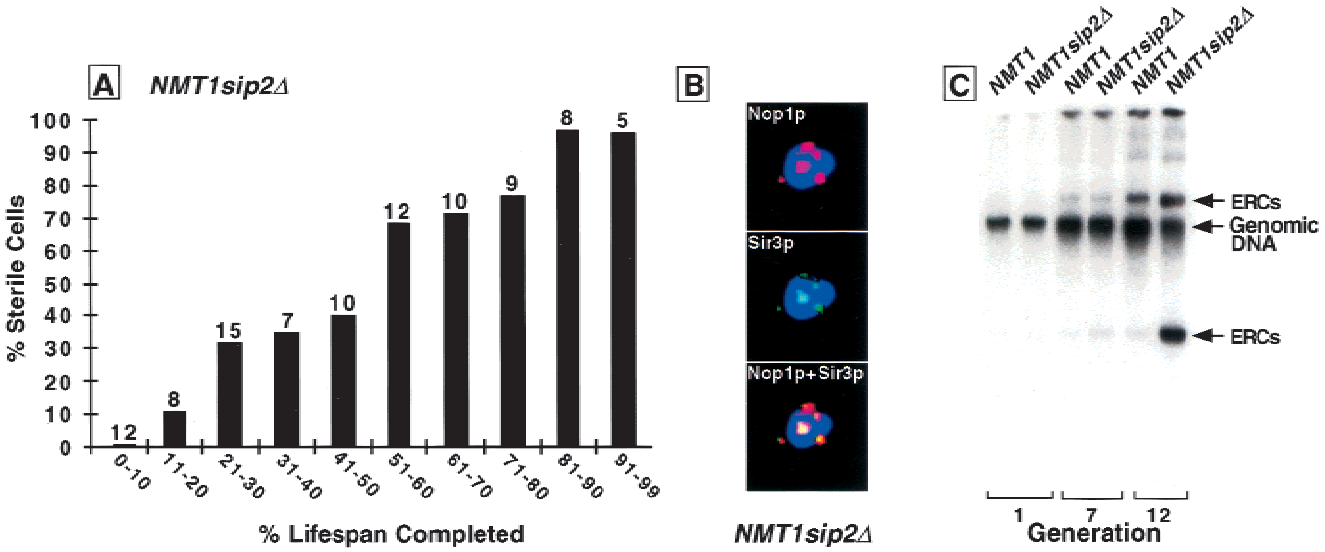

Figure 4. *NMT1sip2Δ* cells undergo rapid aging. (*A*) Sterility assay, performed as described in the legend to Fig. 1B. The shortened lifespan of these cells is accompanied by progressive sterility. (*B*) Multilabel immunohistochemical study of a *sip2Δ* cell at generation 12 (ABSC = 11.8 ± 3.6) showing Sir3p redistribution to a fragmented nucleolus. Note that 20%–25% of generation 12 *sip2Δ* cells exhibit these phenotypic changes (n = 1000 cells/scored per experiment; two independent experiments). (*C*) Increased ERC levels in *sip2Δ* cells. ABSC for the indicated generations were as follows: *NMT1* (0.9 ± 1.1; 7.5 ± 2.8; 12.7 ± 4.1); *NMT1sip2Δ* (0.9 ± 1.1; 7.2 ± 2.3; 11.8 ± 3.6).

actually reduced by generation 7 in this strain (Fig. 6A; below). Therefore, we presume that the decreased lifespan of *NMT1snf1Δ* cells results from deleterious effects unrelated to accelerated aging. Second, removing Snf4p (the activating subunit of the Snf1p complex), reduces Snf1p activity (Jiang and Carlson 1997; Ludin et al. 1998) and leads to a modest increase in longevity: The mean generational lifespan of *NMT1snf4Δ* cells is 110%–120% of wild type.

Next, we tested the hypothesis that *sip2Δ* accelerates aging by producing increased or aberrant cellular Snf1p kinase activity. When a high-copy 2 μ plasmid (YEp24) containing *SNF1* under the control of its own promoter was introduced into wild-type cells, mean generational lifespan decreased to 74% of cells containing vector alone. This reduction was accompanied by sterility, nucleolar fragmentation, and Sir3p redistribution. By generation 7, YEp24–*SNF1* had produced a marked augmentation in ERC concentration so that they were the predominant cellular DNA species (Fig. 6B). In contrast, deletion of *SNF1* from wild-type cells produced a 2-fold reduction in ERC levels by generation 7 (Fig. 6A,B).

YEp24–*SNF1* also caused an additional 25% reduction in the mean lifespan of *sip2Δ* cells whereas the YEp24 vector had no effect. The reduced lifespan of *sip2***Δ**,YEp24–*SNF1* cells was associated with the manifestations of aging, including further increases in ERC levels (data not shown).

Together, these results indicated that *sip2Δ* produces its effect on aging by increasing the activity of Snf1p kinase. Moreover, the mean generational lifespans of isogenic *snf1Δ* and *sip2Δsnf1Δ* strains were the same, consistent with the idea that they operate through a com-

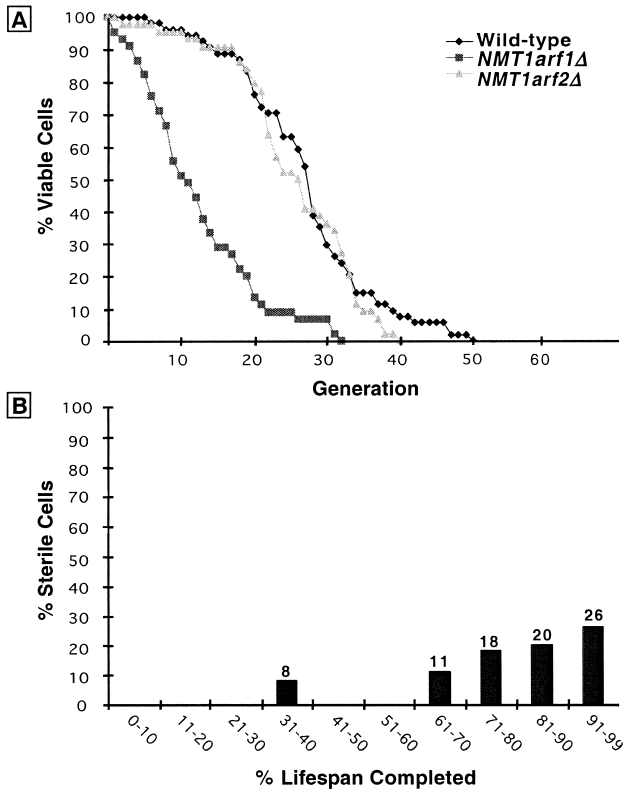

Figure 5. Loss of other N-myristoylproteins produces a shortening of lifespan without accompanying signs of aging or has no effect on lifespan. (*A*) Lifespans of the wild-type strain and isogenic strains containing null alleles of genes encoding two N-myrisotylproteins, Arf1p and Arf2p. (*B*) Sterility assay of *arf1Δ* cells.

Table 1. *Yeast strains*

Strain	Genotype	Source
YB332	*S288CMATa**NMT1ura3-52his3Δ200ade2-101lys2-801leu2-3,112*	Ashrafi et al. 1998
YB336	*S288CMATa**nmt1-451Dura3-52his3Δ200ade2-101lys2-801leu2-3,112*	Ashrafi et al. 1998
YB614	*S288CMATa**NMT1ura3-52his3Δ200ade2-101lys2-801leu2-3,112, snf4::HIS3*	this work
YB616	*S288CMATa**NMT1ura3-52his3Δ200ade2-101lys2-801leu2-3,112, mig1::HIS3*	this work
YB618	*S288CMATa**NMT1ura3-52his3Δ200ade2-101lys2-801leu2-3,112,sip1::HIS3*	this work
YB651	*S288CMATa**NMT1ura3-52his3Δ200ade2-101lys2-801leu2-3,112gal-83::HIS3*	this work
YB670	*288CMATa**NMT1ura3-52his3Δ200ade2-101lys2-801leu2-3,112,sip2::URA3, snf4::HIS3*	this work
YB674	*S288CMATa**NMT1ura3-52his3Δ200ade2-101lys2-801leu2-3,112,sip2::LEU2, snf4::HIS3*	this work
YB810	*S288CMATa**NMT1ura3-52his3Δ200ade2-101lys2-801leu2-3,112,sip2::HIS3*	this work
YO28	*S288CMATa**NMT1ura3-52his3Δ200ade2-101lys2-801leu2-3,112snf1::HIS3*	this work
YO43	*S288CMATa**ura3-52/ura3-52his3Δ200/his3Δ200ade2-101/ade2-101 lys2-801/lys2-801leu2/leu2trp1-901/trp1-901TYR/tyr CAN^S/can^R snf1Δ::URA3*	M. Johnston
YB686	*S288CMATa**ura3-52his3Δ200-ade2-101lys2-801leu2trpl-901TYRCAN^{S}sip2Δ::HIS3*	this work
YB687	*S288CMATa**ura3-52his3Δ200ade2-101lys2-801leu2trp1-901TYRCAN^{S}snf1Δ::URA3*	this work
YB688	*S288CMATa**ura3-52his3Δ200ade2-101lys2-801leu2trp1-901TYRCAN^{S}sip2Δ::HIS3 snf1Δ::URA3*	this work
YO36	*W303-1AMATa**ura3-1his3-11,15ade2-1leu2-3,112can1-100trp1-1*	Sinclair et al. 1997
YO40	*W303-1AMATa**ura3-1his3-11,15ade2-1leu2-3,112can1-100trp1-1, sip2::URA3*	this work

mon pathway. However, caution must be exercised when interpreting results obtained with this double mutant because cells with *snf1Δ* are "sick" and have a reduced lifespan that is not accompanied by the manifestations of aging. Therefore, we created a *NMT1sip2Δsnf4Δ* strain as an additional test of the hypothesis that *sip2Δ* affects aging by increasing Snf1p kinase. We reasoned that if *sip2Δ* results in increased kinase activity, then the effect of this increase should be countered by removal of Snf1p's coactivator, Snf4p. The results support the hypothesis. The mean generational lifespans of two independently generated *sip2Δsnf4Δ* strains (YB670 and YB674 in Table 1) were twice that of isogenic *sip2Δ* cells (31–33 vs. 15, respectively), and equivalent to *snf4Δ* cells (110%–120% of wild type) (Fig. 7).

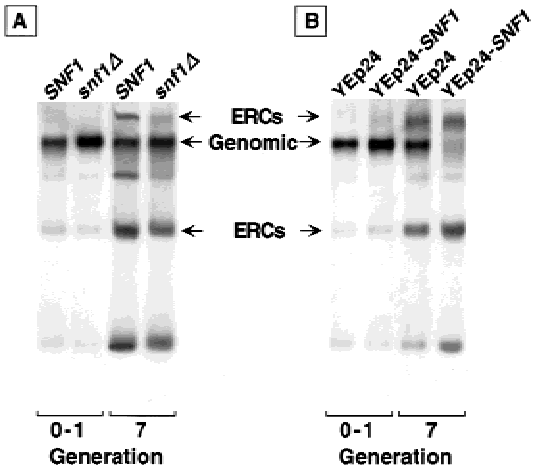

Figure 6. ERC accumulation is reduced when Snf1p is deleted and augmented when Snf1p is overexpressed. Southern blot analysis of ERC accumulation in the indicated strains at generation 0–1 (ASBC = 0.9 ± 1.1) and at generation 7 (ASBC = 7.3 ± 2.6). Equal amounts of total cellular DNA were applied to all lanes. Note that in generation 7 wild-type cells containing YEp24–*SNF1*, the signal produced from hybridization of the labeled rDNA probe with ERCs, is >80% of the signal produced by reaction of the probe with total cellular DNA.

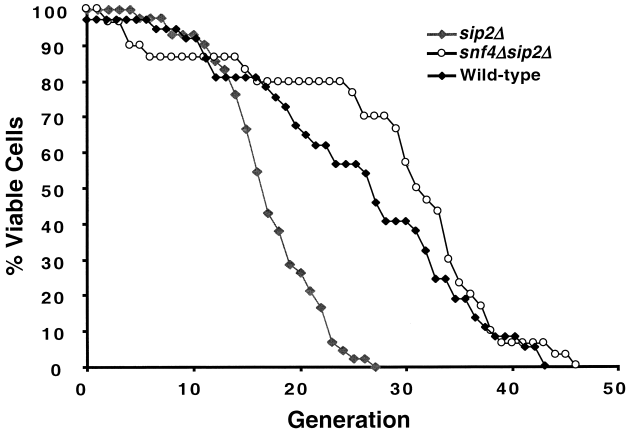

Figure 7. Removal of the Snf1p activator, Snf4p, rescues the reduced lifespan of *sip2Δ* cells. Strains YB810 (*sip2Δ*) and YB674 (*sip2Δsnf4Δ*) were derived from a S288C parent (YB322; see Table 1).

Changes in the intracellular location of Mig1p provide support for generational increases in Snf1p kinase activity

Mig1p is a zinc finger transcription factor responsible for most of the repression of glucose-repressed genes in yeast (Nehlin and Ronne 1990; Nehlin et al. 1991; for review, see Johnston 1999). In wild-type cells, Mig1p resides in the nucleus when glucose is present. In the absence of glucose, Snf1p phosphorylation of Mig1p results in redistribution of the protein from the nucleus to the cytoplasm (DeVit et al. 1997).

We monitored the intracellular location of a Mig1p–green fluorescent protein (GFP) chimera expressed in wild-type S288C and W303 strains (YB332 and YO36 in Table 1), and in YB322-derived *sip2Δ* cells, during growth in YPD medium (glucose = 110 mM). At generation 0–1, Mig1p–GFP is detectable in the cytoplasm in <1% of wild-type and *sip2Δ* cells (n = 2–3 experiments/strain; Fig. 8A). In the two wild-type strains, this value remains essentially unchanged at generation 5–6 (0%–5%). By generation 11–12, 25% of cells (range = 24%–34%, n = 3 experiments) display cytoplasmic localization despite continuous exposure to glucose-rich medium prior to and throughout the sorting steps used for their recovery, and during fluorescence microscopy (Fig. 8A). Remarkably, 10%–23% of *sip2Δ* cells exhibit cytoplasmic Mig1p–GFP as early as generation 4–5. This value increases to 58%–95% by generation 11–12 (n = 2 experiments) (Fig. 8A).

A trivial explanation for the age-associated redistribution of Mig1p–GFP would be proteolytic release of its GFP domain rather than increased Snf1p-dependent phosphorylation of its Mig1p domain. Therefore, Western blots containing total cellular proteins from generation 0–1 and generation 7 wild-type and *sip2Δ* cells were probed with antibodies to GFP. An immunoreactive band of the expected mass for Mig1p–GFP was observed in young and old wild-type and *sip2Δ* cells and was absent from control cells that lacked the MIG1–GFP plasmid (Fig. 8B). The intensity of this band did not diminish with increasing age in *sip2Δ* cells, nor did a band appear corresponding to GFP alone (Fig. 8B). These results indicate that there is no appreciable cleavage of Mig1p–GFP as cells age.

We can not formally rule out the possibility that the generation-associated redistribution of Mig1p–GFP from the nucleus to the cytoplasm reflects as yet unknown effects of aging on the activity of one or more cellular phosphatases, or on the nuclear import/export machinery itself. However, two findings from previous studies of Mig1p localization in vegetatively growing cells (Dewit et al. 1997; Dewit and Johnston 1999) support our hypothesis that Snf1p mediates Mig1p translocation in aging cells. First, Mig1p is not observed in the cytoplasm of log-phase cells in the absence of Snf1p. Second, Mig1p contains four putative Snf1p phosphorylation sites, two within its nuclear export signal sequence. The number of log-phase cells that contain cytoplasmic Mig1p decreases as more of these sites are mutated: Negligible

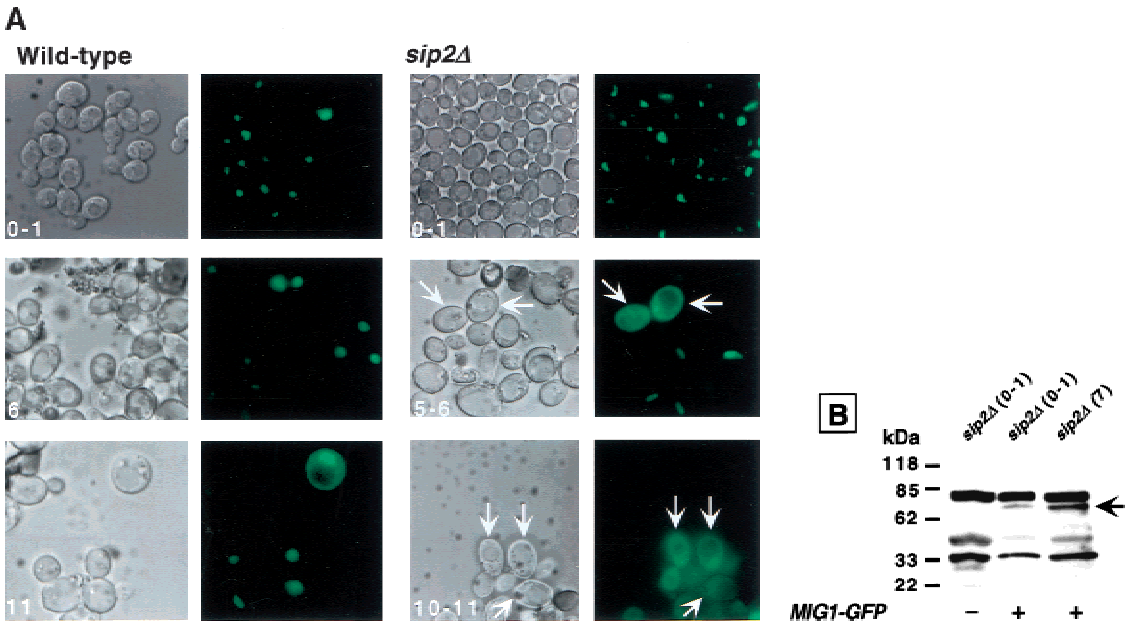

Figure 8. The cytoplasmic localization of a Mig1p–GFP fusion protein provides in vivo evidence for enhanced Snf1p kinase activity in *sip2Δ* cells. (*A*) Wild type and *sip2Δ* containing a *CEN* plasmid encoding Mig1p–GFP were sorted to the generations indicated. The intracellular distribution of Mig1p–GFP was then determined using fluorescence microscopy. Nomarski and fluorescence images of each field are shown. Arrows point to examples of cells where Mig–GFP is predominantly cytoplasmic. See text for further discussion. (*B*) Western blot of total cellular proteins isolated from young and old *sip2Δ* cells without (–) and with (+) a *MIG1–GFP* plasmid. Cells were recovered at the generational ages noted in parenthesis. The blot was probed with a GFP monoclonal antibody. The arrow points to the Mig1p–GFP fusion protein.

cytoplasmic Mig1p is observed when all of these sites are eliminated (DeVit and Johnston 1999).

Finally, because *mig1Δ* cells have a normal lifespan (data not shown), we concluded that Mig1p is not responsible for expression of the *sip2Δ* phenotype, or an essential regulator of aging.

Biochemical studies of glucose uptake and metabolism in sip2Δ *compared to wild-type cells*

Snf1p acts as a nutrient sensor in the cell, coupling glucose availability to gene expression. Snf1p activity is upregulated when cells are starved or otherwise stressed (Hardie et al. 1998). Therefore, a series of biochemical assays were performed to determine whether there are changes in glucose uptake and metabolism as a function of generational age and *SIP2* allele.

Direct measurements of intracellular glucose levels revealed no statistically significant differences between wild-type and *sip2Δ* cells cultured in YPD medium. This similarity was evident when young (generation 0–1) cells were compared with one another (4.9 ± 0.8 vs. 3.8 ± 1 fmole/cell for wild type and *sip2Δ*, respectively), and with older cells (4.7 ± 1.7 and 6.1 ± 0.5 fmole/cell for generation 6 wild type and generation 4 *sip2Δ*; 10^6 cells assessed/genotype/generational time point/assay; $n = 4$).

Hexokinase catalyzes the first step in glycolysis, the conversion of glucose to glucose-6-phosphate (G6P). Sensitive microanalytic methods (Passonneau and Lowry 1993) were used to measure hexokinase activity in individual wild-type and *sip2Δ* mother yeast cells to determine whether aging is associated with changes in the ability of glucose to enter the glycolytic pathway. Individual cells were harvested directly from YPD/agar plates by micromanipulation ($n = 9$–21 individual mothers assayed/age/genotype). Hexokinase activity increases progressively as wild-type mothers progress from generation 0–1 to generation 19–21. Hexokinase activity in *sip2Δ* mothers rises more abruptly, to higher levels at earlier generations (Fig. 9A).

Virtually identical age- and genotype-associated differences in hexokinase activity were documented in lysates prepared from populations of 2×10^4 wild-type and *sip2Δ* cells that had been recovered at various ages by sorting (data not shown). This result provided evidence that the sorting procedure does not produce artifactual changes in cellular glycolytic activity.

Microanalytic methods were then used to measure directly the product of hexokinase, G6P, in lysates representing 5×10^4 sorted cells. Levels of G6P correlated directly with the generational age- and *SIP2* allele-associated differences noted in hexokinase activity. In wild-type cells, G6P levels increase 2.1-fold from generation 0–1 to generation 6 (i.e., from 21.8 ± 3 to 45.1 ± 7 amole/cell; $P < 0.05$). G6P levels in generation 0–1, 4, and 6–8 *sip2Δ* cells were 1.4-fold, 4.5-fold, and 5.3-fold higher than in the reference generation 0–1 wild-type cells ($P < 0.05$ for generations 4 and 6–8).

Like glucose, 2-deoxyglucose (2DG) is a substrate for cellular glucose transporters and hexokinase. 2-deoxyglucose-6-phosphate (2DG6P) does not undergo rapid metabolic processing: For example, it takes 5000-fold more G6P dehydrogenase to oxidize 2DG6P than G6P (Passonneau and Lowry 1993). Therefore, changes in cellular 2DG6P levels after exposure to exogenous 2DG can be used as a reporter of 2DG uptake (and hexokinase activity).

Young and older wild-type and *sip2Δ* cells were incubated with 110 mM glucose for 20 min, followed by the addition of 0.1 mM 2DG. Aliquots were removed 5, 10, and 20 min after 2DG was added, and cellular 2DG6P levels were measured (see Materials and Methods). A similar progressive increase in 2DG6P occurs in young wild-type and *sip2Δ* cells (Fig. 9B). Moreover, there is no impairment in the uptake of 2DG and its conversion 2DG6P in older *sip2Δ* cells. The greater rate of accumulation of 2DG6P observed in older compared to younger cells (Fig. 9B) can be explained, at least in part, by their increased hexokinase activity.

These assays of cellular glucose, G6P and 2DG6P levels, and hexokinase activities indicate that a generational increase in Snf1p kinase activity can not be attributed to age-associated reductions in cellular glucose import, or to detectable defects in the ability of glucose to enter the glycolytic pathway. The observed generational increases in hexokinase and G6P prompted us to measure ATP and nicotinamide-adenine dinucleotide (NAD^+) levels in wild-type and *sip2Δ* cells. The results disclosed that as wild-type cells proceed from generation 0–1 to generation 6 in medium containing 110 mM glucose they store energy. Cellular ATP content increases 2.6-fold from 64 ± 7.5 to 146.0 ± 21.5 amole/cell ($P < 0.05$; Fig. 9C), while NAD^+ rises a modest 20% (Fig. 9D). *sip2Δ* cells store energy to a significantly greater extent: ATP content is 2.3-fold higher in young *sip2Δ* cells compared to young wild-type cells, and 4.3-fold higher at generation 4; NAD^+ content is 1.7- and 2.8-fold higher, respectively (Fig. 9C,D).

Figure 9E summarizes the impressive correlation between fold-changes in hexokinase activity, G6P, ATP, and NAD^+ as a function of generational age and *SIP2* allele. It is important to note that as yeast cells age, their size increases. Therefore, increases in G6P, ATP, and NAD^+ content may not necessarily be accompanied by increases in their molarity. To address this point, we defined the sizes of generation 0–1 and 7 *sip2Δ* cells ($n = 90$/group) by measuring their two-dimensional areas in photographs directly, and then calculating their volumes. The results revealed a 40% increase over the course of seven generations. The magnitude of this calculated increase is less than the increase in G6P, ATP, and NAD^+ content documented as *sip2Δ* cells progress from generations 0–1 to 4–6, suggesting that the molarity of these compounds rises.

In summary, our findings indicate that changes in glucose metabolism are a manifestation of aging in wild-type yeast cells, and that this process is exaggerated in the more rapidly aging *sip2Δ* cells. As discussed below, these findings have implications concerning mechanisms that may underlie the relationship between calorie restriction, energy storage, and aging.

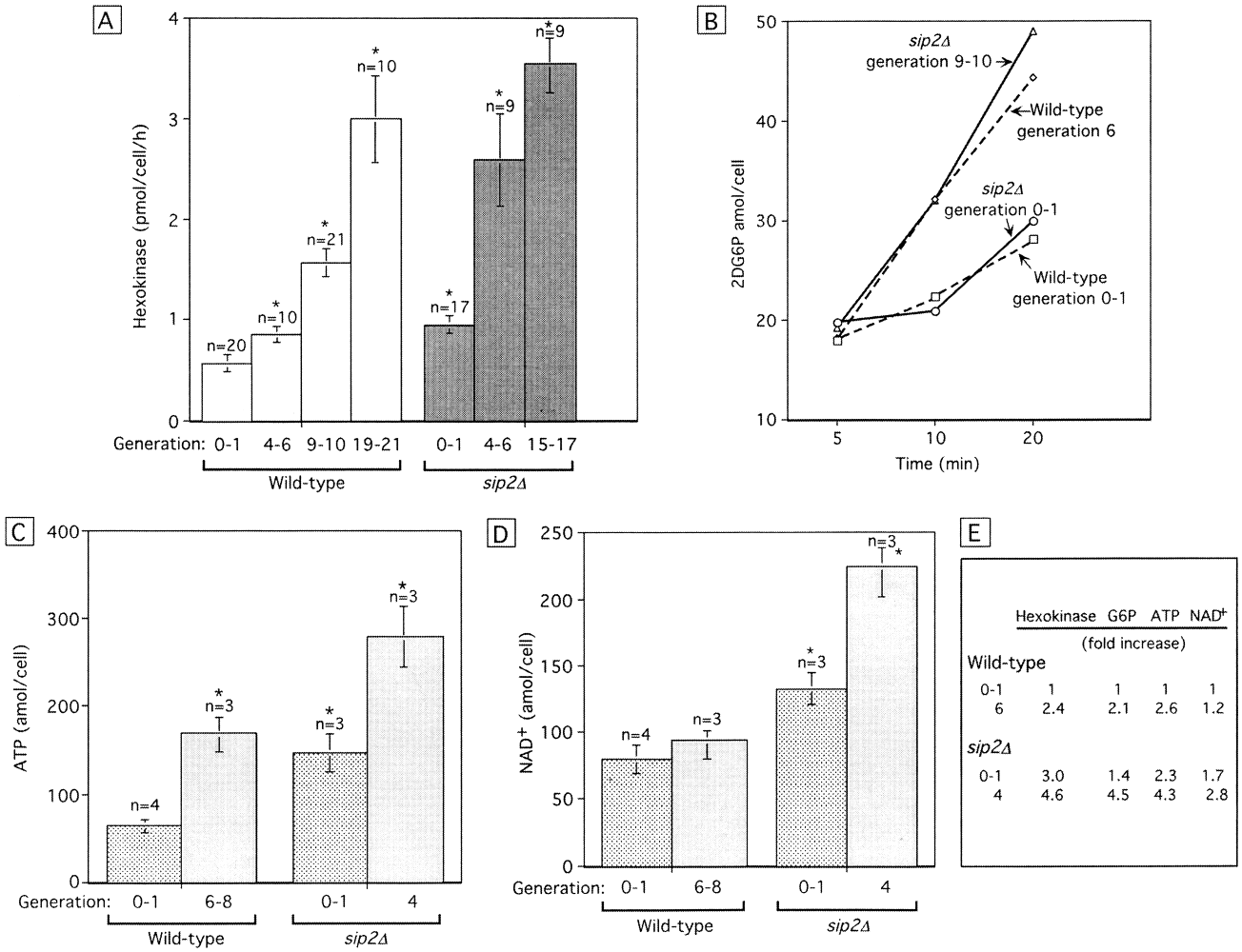

Figure 9. The rapid aging of *sip2Δ* cells is accompanied by increases in hexokinase activity and energy storage. (*A*) Hexokinase activity was measured in lysates prepared from individual mothers recovered at the indicated generations. Mean values ± 1 S.D. are plotted. (Asterisk) Values are significantly different ($P < 0.05$; Student's t-test) from generation 0–1 wild-type cells. (*B*) 2DG6P accumulation as a function of time in isogenic wild-type and *sip2Δ* cells. (*C,D*) Cellular ATP and NAD^+ levels. The number of independently generated lysates/cell population/generational time point is noted ($n = 50{,}000$ cells assayed/lysate/experiment). Note that generation 4 in *sip2Δ* cells and generation 6–8 in wild-type cells represent equivalent fractions of their total lifespans. (*E*) Summary of fold differences in hexokinase, G6P, ATP, and NAD^+ levels relative to young wild-type cells.

Discussion

The significance of mutations that produce a shortened lifespan must be viewed with caution. Proof that a mutation is actually affecting an aging-related pathway should include evidence that shortening of the generational lifespan is accompanied by other known stigmata of aging, and evidence that opposing genetic manipulations leads to increased lifespan. We believe that our genetic analysis of *SIP2* and its associated Snf1p-kinase pathway satisfies these requirements. The shortening of lifespan observed in *nmt1–451DSIP2* and *NMT1sip2Δ* strains is accompanied by all of the currently defined manifestations of aging in *S. cerevisiae*. This is in contrast to results obtained with other N-myristoylproteins selected in our screen, and with other members of the Snf1p kinase pathway. Deletion of some of these genes produce a shortening of lifespan without any accompanying signs of aging (e.g., *arf1Δ*, *sip1Δ*) or have no effect on mean generational lifespan (e.g., *arf2Δ*, *gal83Δ*, *mig1Δ*).

We have found that manipulating Snf1p-kinase activity affects aging in yeast. Forced expression of *SNF1* in wild-type cells shortens lifespan and evokes all the known aging phenotypes, whereas deleting *SNF4* (encoding the activating subunit of the Snf1p complex) extends lifespan. Moreover, removal of Sip2p accelerates aging through a Snf1p kinase-dependent mechanism: the rapid aging phenotype of *sip2Δ* cells is rescued completely by introduction of a *snf4Δ* mutation. The lifespan results obtained for *snf1Δ* and *sip2Δsnf1Δ* cells are difficult to interpret as complete removal of Snf1p results in loss of cellular fitness. This loss of fitness is not surprising because Snf1p is responsive to multiple cellular stresses,

has multiple substrates, and hence is likely to have pleiotropic effects. Therefore, some activities of Snf1p may affect fitness without impacting aging. Removal of Snf4p simply attentuates Snf1p activity, thereby allowing assessment of the role of Snf1p in aging.

Yeast two-hybrid assays have established that Sip2p binds to Snf1p (Yang et al. 1994). In vitro kinase activity is not affected demonstrably by Sip2, but only a limited number of substrates have been tested (Yang et al. 1994). Previous genetic studies suggest that Sip2p, Gal83p, and Sip1p mediate interactions between Snf1p and distinct targets (Yang et al. 1994; Vincent and Carlson 1999). Based on our findings, we speculate that Sip2p inhibits phosphorylation of one or more cellular proteins/enzymes by Snf1p that normally affect aging. Alternatively, Sip2p may regulate production of Snf1p substrates or their interactions with the kinase. Removing Sip2p leads to an increase in Snf1p kinase activity, a conclusion supported by the augmented generational increase in Snf1p phosphorylation-dependent translocation of Mig1p from the nucleus to the cytoplasm of *sip2Δ* cells.

Snf1p is required for induction of glucose-repressed genes in response to glucose starvation. Therefore, it is intriguing that Snf1p activity increases as cells age, even when there is abundant glucose in the environment. Our measurements of intracellular glucose concentrations and of 2-deoxyglucose uptake indicate that aging wild-type and *sip2Δ* cells have no detectable defects in their ability to abstract glucose from the environment. Remarkably, the initial step in glycolysis, hexokinase-catalyzed conversion of glucose to G6P, increases as cells age, as does cellular ATP content. These effects are more pronounced in *sip2Δ* compared with wild-type cells.

The augmentation in cellular ATP content is also consistent with our proposed age-associated increase in Snf1p activity. The mammalian homolog of Snf1p, AMP-activated kinase (AMP-K), functions as a fuel guage to help conserve energy when cells are starved. AMP-K is known to phosphorylate, and thereby inactivate, a series of ATP-utilizing enzymes, resulting in retention of energy sources. These enzymes include acetylCoA carboxylase, and HMG CoA reductase, the critical regulator of isoprenoid and sterol biosynthesis. For example, inhibition of acetyl-CoA carboxylase can promote ATP conservation in two ways: (1) by turning off the ATP-consuming fatty acid biosynthetic pathway, and (2) by turning on the ATP-generating fatty acid oxidation pathway (for review, see Hardie et al. 1998). Like AMP-K, purified yeast Snf1p complex phosphorylates and inactivates (yeast) acetyl-CoA carboxylase (Acc1p; Mitchelhill et al. 1994).

Our biochemical analyses, which indicate that aging in yeast is marked by a shift in metabolism towards increased energy pools, are consistent with results obtained from DNA microarray studies of gene expression in the skeletal muscles of young and old mice (Lee et al. 1999). A persistent theme in the study of aging is the close connection between regulation of energy intake and expenditure, and longevity. Many organisms, including *S. cerevisiae*, *C. elegans*, and mice can alter their rate of aging in response to changes in nutrient availability (Klass and Hirsch 1976; Ashrafi et al. 1999; Lee et al. 1999). In *C. elegans*, an insulin-like signaling pathway controls entry into diapause when nutrients are limited during the larval stage. This pathway also affects longevity during the adult stage (Kenyon et al. 1993; Kimura et al. 1997; Wood 1998).

In a recent study, Guarente and coworkers speculated that NAD^+ may serve as an indicator of cellular nutritional status and help regulate aging (Imai et al. 2000). They discovered that Sir2p, which mediates transcriptional silencing, suppresses ERC formation and extends generational lifespan, and is a NAD-dependent histone deacetylase. They postulated that increases in NAD^+ may promote Sir2p-mediated deacetylation, resulting in enhanced genomic stability and suppression of potentially deleterious patterns of gene expression (Imai et al. 2000). Our biochemical studies establish that as cells age there is a concommittent increase in NAD^+ content. Because increased NAD^+ would be expected to enhance Sir2p-mediated histone deacetylase activity, the increase may be a response designed to help oppose genomic instability. It appears that genomic instability associated with aging in yeast can not be attributed simply to lowered total cellular NAD^+ levels leading to decreased Sir2p histone deacetylase activity. A future challenge will be to determine whether the increased cellular NAD^+ pools are accessible to Sir2p.

Snf1p, Sip2p, and their associated signaling pathway(s) can now be added to a very short list of molecules known to functionally link adaptations to changes in carbon source availability and aging. Our data indicate that Snf1p activity is increased despite abundant nutrients in the environment and that aging is associated with an alteration in cellular energy homeostasis. We propose that the context in which energy accumulation occurs may help determine its impact on the aging process. One interpretation of the accelerated aging phenotype of *sip2Δ* cells is that activation of Snf1p at early generational ages causes premature and inappropriate accumulation/compartmentalization of energy reserves and that the cells are not equipped to deal with these reserves. It will be important to use the microanalytic approaches described in this report to obtain a more comprehensive view of cellular glucose metabolism as yeast cells age. For example, do changes in Snf1p kinase activity correlate with changes in fructose 1,6 bisphosphatase, the enzyme that is increased in calorically restricted mice (Lee et al. 1999) and which drives glycolysis backward to G6P?

As noted above, Sip2p is unique among Snf1p's partners in affecting aging: Neither *gal83Δ* or *sip1Δ* produce a demonstrable effect, suggesting partner-specific effects on phosphorylation. Therefore, identifying the protein targets of this kinase in the presence or absence of Sip2p (or in presence or absence of Sn4p) should provide additional clues about the molecular mechanisms that regulate longevity, and help identify the contexts in which these mechanisms operate.

In summary, *S. cerevisiae* provides an attractive, ge-

netically manipulatable, unicellular, replicative eukaryotic model for deciphering the details about how cellular (and organismal) energy metabolism changes as a function of generational lifespan and Snf1p complex activity. The results should form a framework for designing and interpreting genetic and biochemical tests of whether and how these processes operate in multicellular organisms.

Materials and methods

Strains

The strains used for this study are listed in Table 1. ORFs were deleted in the haploid wild-type strains YB332 or YO36, and replaced with *HIS3*, *URA3*, or *LEU2* markers using a protocol described previously (Baudin et al. 1993). Deletions were confirmed by PCR using allele-specific primers. To generate a *snf1Δsip2Δ* strain, a *sip2Δ* allele was engineered in the diploid strain YO43 (*snf1Δ*; kindly supplied by Mark Johnston, Washington University, Seattle) using the *SIP2::HIS3* fragment employed for generation of strain YB810 (Table 1). Standard methods were used for selecting transformants, sporulation and subsequent tetrad analysis. *sip2Δsnf1Δ* cells were identified by scoring for growth on selective media and by allele-specific PCR.

Mean lifespan determination

Micromanipulation assays (Mortimer and Johnston 1959; Kennedy et al. 1995) were used to define the number of divisions that individual mothers underwent on YPD (1% yeast extract, 2% peptone, 2% dextrose)/agar plates at 24°C. Each experiment involved an analysis of 50–100 mothers of a given genotype. Wild-type cells were always used as internal controls. The statistical significance of observed differences in the lifespans of strains was evaluated using the nonparametric Wilcoxen signed rank test.

Preparation of old-cell populations by sorting

Cells were obtained with an average generational age of seven using the technique described by Smeal et al. (1996). Briefly, 2×10^8 cells were harvested from a mid-log phase culture grown in YPD at 24°C. Cells were washed in phosphate buffered saline (PBS) and then resuspended in 1 ml of PBS containing 7 mg of EZ-link Sulfo-NHS-LC-LC biotin [sulfosuccinimidyl-6′-(biotinamido)-6-hexanamido hexanoate; Pierce]. Following gentle shaking for 15 min at 24°C, unbound biotin was removed by washing cells in PBS (four washes; 1 ml each). Cells were resuspended in 1 liter of YPD (containing 2.5% dextrose), grown at 24°C to an OD_{600} = 0.8, recovered by centrifugation (8 min at 4400*g*), and resuspended in 35 ml PBS containing streptavidin conjugated to magnetic beads (PerSeptive Biosystems; final concentration = 70 μg/ml). The mixture was incubated for 2 hr at 4°C in a polypropylene tube, with brief swirling every 15 min. Biotin-coated cells that had bound to magnetic beads were recovered with a magnetic sorter and washed eight times in ice cold YPD, with magnetic sorting after each wash. Average bud scar count (ABSC) of the sorted cell population was determined by staining an aliquot of the cells with fluorescent brightener 28 (Sigma) and counting the number of bud scars per cell with a fluorescence microscope (n = 40–70 cells analyzed/preparation).

Generation 0–1 refers to the population of cells that remained after old cells had been removed by magnetic sorting. On average, 50% of cells in this population are newly formed daughters, 25% are mothers that have undergone one division, 12.5% are mothers that have undergone two divisions, etc.

To obtain a population that had undergone an average of 12–14 divisions, 10^8-sorted generation 7 cells were resuspended in 1 liter YPD (containing 2.5% dextrose) and incubated at 24°C for an additional 13 hr. A second sort was then performed exactly as above.

Defining the localization of Mig1p–GFP in aging cells

YB332, YO36 (wild type), and YB810 (*sip2Δ*) cells were transformed with pBM3315, a *CEN* plasmid containing *MIG1–GFP* under the control of the *MIG1* promoter (DeVit et al. 1997; a gift from Mark Johnston, Washington University). Cells were sorted as above and the intracellular location of Mig1–GFP was defined by fluorescence microscopy ($n \geq 100$ cells scored/generational time point/experiment; n = 2–3 independent experiments/strain). Exposure to glucose (2% w/v) was maintained throughout the sorting and microscopy steps.

To assess the integrity of Mig1–GFP, lysates were prepared from wild-type and *sip2Δ* cells recovered at generations 0–1 and 7. Cellular proteins were fractionated by SDS-PAGE and transferred to PVDF membranes (Millipore). Blots were probed with a mouse monoclonal anti-GFP (Zymed; final dilution = 1:1000). Antigen-antibody complexes were visualized using reagents and protocols contained in the enhanced chemiluminescence kit from Tropix.

Immunohistochemistry

Sir3p distribution was defined as follows. Cells ($5–50 \times 10^6$) were washed twice in PBS, resuspended in 1 ml of 0.1 M EDTA (pH 8)/10 mM DTT, and incubated for 10 min at 30°C with gentle shaking. Cells were recovered by centrifugation, and washed in 1 ml YPD/20% (w/v) sorbitol. Spheroplasts were prepared by adding Zymolyase-100 (ICN, 100 U/mg; final concentration = 6 μg/ml) and incubating the cells at 30°C for 15–60 min (depending on the strain). Spheroplasts were recovered, washed, and resuspended in 1 ml of YPD/20% sorbitol and then fixed for 20 min in 3.7% formaldehyde. Fixed spheroplasts were resuspended in 200 μl YPD, placed on Vectabond-coated glass slides (Vector Laboratories), air dried for 10–15 min, treated for 6 min with methanol (–20°C) followed by acetone (1 min; –20°C) and then preincubated for 1 hr in blocking buffer [PBS/1% bovine serum albumin (BSA)/0.1% Triton X-100]. Antibodies were added in the following order (all diluted 1:100 in blocking buffer, all incubations at 37°C): (1) rabbit anti-Sir3p, overnight incubation (Sinclair et al. 1997; kindly supplied by L. Guarente, Department of Biology, MIT); (2) fluorescein isothiocyanate (FITC)-conjugated goat anti-rabbit IgG, 1 hr incubation (Vector Laboratories); (3) mouse monoclonal antibodies to yeast fibrillarin, overnight incubation (Nop1p, Sinclair et al. 1997; from L. Guarente); and (4) indocarbocyanine (Cy3)-tagged goat anti-mouse IgG, 1 hr incubation (Sigma). DNA was stained blue with 4′,6′-diamidino-2-phenylindole. Staining patterns were scored for a minimum of 500–1000 cells/genotype/experiment.

ERC analysis

DNA was prepared according to Sinclair and Guarente (1997) and fractionated by electrophoresis for 30 hr through 0.7% agarose containing TAE buffer (40 mM Tris acetate, 1 mM EDTA at pH 7.5) at constant voltage (1 volt/cm gel length with buffer recirculation at room temperature). Following capillary transfer to GeneScreen Plus (NEN Life Science Products), blots were probed with a ^{32}P-labeled, 2.8-kb *Eco*RI fragment containing

rDNA sequences obtained from pNL47 (Sinclair and Guarente 1997). Relative ERC levels were defined by analyzing the blot with a storage phosphorimaging system (Molecular Dynamics).

Biochemical assays of young and old cell populations

The principles underlying these well-established microanalytic techniques have been described in great detail by Lowry and coworkers (e.g., Lowry 1980; Passonneau and Lowry 1993) and are based on highly specific enzymatic reactions where a pyridine nucleotide is either oxidized or reduced. Great sensitivity is achieved by amplifying the nucleotide product several thousand-fold by enzymatic cycling. These techniques have been used to measure glucose, G6P, 2DG6P, ATP, NAD^+, and hexokinase in a wide variety of higher eukaryotic cells (e.g., Chi et al. 1988; Manchester et al. 1994).

Young or older cells (recovered by sorting at 4°C) were incubated at 24°C in YPD for 20 min, pelleted, rinsed in PBS, quickly frozen in liquid nitrogen, and freeze-dried for four days at –35°C. For some experiments, cells were incubated with YPD containing 0.1 mM 2-deoxyglucose. In all cases, aliquots were removed prior to pelleting and cell-number defined with a hemocytometer.

To prepare samples for measurement of glucose, G6P, 2DG6P, ATP, and NAD^+ levels, 100 µl of 0.02 M HCl were added to 10^7 freeze-dried cells. The mixture was incubated at 80°C for 20 min to lyse cells, and to destroy endogenous enzymes (e.g., hexokinase), as well as reduce pyridine nucleotides. The extract was neutralized by adding 100 µl 100mM Tris-HCl (pH 8.1) containing 0.02 N NaOH, and then stored at –20°C prior to assay.

To prepare samples for hexokinase assay, 10^7 freeze-dried cells were incubated for 1 min at 24°C in 1 ml of extraction buffer (20 mM phosphate buffer at pH 7.4, 0.02% BSA, 0.5 mM EDTA, 5 mM β-mercaptoethanol, 25% glycerol, and 0.5% Triton X-100). Extracts were stored at –70°C.

To measure hexokinase activity in individual yeast cells grown on YPD/agar, cohorts of mothers were microdissected from their daughters as they underwent successive rounds of cell division. Individual mothers were picked from the plate using a subnanoliter capacity quartz constriction micropipet and transferred to 0.5 µl of extraction buffer under oil in a telfon rack (Passonneau and Lowry 1993). Following a 1 hr incubation at 20°C, the rack, containing all samples (1 mother/well; n = 9–21 mothers/generational time point), was placed under house vacuum, and the vacuum chamber stored at –80°C.

To begin the hexokinase assay, samples were thawed (and lysed) at 20°C. Hexokinase reaction buffer (0.1 µl) [200 mM Tris-HCl at pH 8.1, 0.1% BSA, 14 mM $MgCl_2$, 10 mM ATP, 10 mM glucose, 1 mM DTT, 20 µM NADP, 1% Triton X-100, 2 µg/ml glucose-6-phosphate dehydrogenase from *Leuconostoc mesenteroides* (specific activity = 312 units/mg protein; Calbiochem)] was combined with a 0.1 µl aliquot of the individual cell lysate. The mixture was incubated for 1 hr at 20°C. The reaction was then stopped and excess NADP was destroyed by adding 0.1 µl 0.25 N NaOH and incubating the solution at 80°C for 20 min. Once the rack had cooled to room temperature, 5 µl of NADP cycling reagent was added [100 mM imidazole-HCl at pH 7.0, 2 mM G6P (Sigma), 7.5 mM disodium α-ketoglutarate (Sigma), 0.1 mM ADP, 25 mM ammonium acetate, 0.1% BSA, 1.5 units/ml glutamate dehydrogenase (Boehringer), and 1.5 U/ml of *Leuconostoc mesenteroides* G6P dehydrogenase]. The mixture was incubated for 1 hr at 38°C. The cycling reaction was stopped by adding 0.5 µl of 1 N NaOH and incubating the solution at 80°C for 20 min. A 5-µl aliquot was removed and added to 1 ml of 6-phosphogluconate indicator reagent [100 mM imidazole-HCl at pH 7.0, 30 mM ammonium acetate, 2 mM $MgCl_2$, 0.1 mM EDTA, 0.1 mM NADP, and 0.1 units/ml 6-phosphogluconate dehydrogenase (Boehringer)]. The NADPH product generated from NADP was measured fluorimetrically. For each experiment, G6P standards were assayed in parallel reactions and used as a reference to compute hexokinase activity in individual cell lysates. Two independent standards were also employed: A NADP standard was incorporated at the cycling step to mimic the G6P standards, and a 6-phosphogluconate standard was assayed to validate the G6P and NADP standards.

Acknowledgments

We are indebted to David Sinclair, Kevin Mills, Pierre Defossez, Leonard Guarente, and Mark Johnston for generously providing reagents and protocols, and for their many helpful comments. We also thank Michael Khodadoust and Thalia Farazi for their invaluable assistance at various stages of this study. This work was supported by grants from the National Institutes of Health (AI38200) and the American Federation for Aging Research (predoctoral fellowship to K.A.).

The publication costs of this article were defrayed in part by payment of page charges. This article must therefore be hereby marked "advertisement" in accordance with 18 USC section 1734 solely to indicate this fact.

References

Alepuz, P.M., Cunningham, K.W., and Estruch, F. 1997. Glucose repression affects ion homeostasis in yeast through the regulation of the stress-activated *ENA1* gene. *Mol. Microbiol.* **26:** 91–98.

Arking, R. 1998. *Biology of Aging* (2nd Edition). Sinaur Associates, Sunderland, MA.

Arking, R., Buck, S., Berrios, A., Dwyer, S., and Baker, G.T., III. 1991. Elevated paraquat resistance can be used as a bioassay for longevity in a genetically based long-lived strain of *Drosophila. Dev. Genet.* **12:** 362–370.

Ashrafi, K., Farazi, T.A., and Gordon, J.I. 1998. A role for *Saccharomyces cerevisiae* fatty acid activation protein 4 in regulating protein *N*-myristoylation during entry into stationary phase. *J. Biol. Chem.* **273:** 25864–25874.

Ashrafi, K., Sinclair, D., Gordon, J.I., and Guarente, L. 1999. Passage through stationary phase advances replicative aging in *Saccharomyces cerevisiae. Proc. Natl. Acad. Sci.* **96:** 9100–9105.

Baudin A., Ozier-Kalogeropoulos, O., Denouel, A., Lacroute, F., and Cullin, D. 1993. A simple and efficient method for direct gene deletion in *Saccharomyces cerevisiae. Nucleic Acids Res.* **21:** 3329–3330.

Bhatnagar, R.S. and Gordon, J.I. 1997. Understanding covalent modification of proteins by lipids: Where cell biology and biophysics mingle. *Trends Cell Biol.* **7:** 14–18.

Bhatnagar, R.S., Futterer, K., Farazi, T.A., Korolev, S., Murray, C.L., Jackson-Machelski, E., Gokel, G.W., Gordon, J.I., and Waksman, G. 1998. Structure of N-myristoyltransferase with bound myristoyl CoA and peptide substrate analogs. *Nature Struct. Biol.* **5:** 1091–1097.

Boutin, J.A. 1997. Myristoylation. *Cell. Signal.* **9:** 15–35.

Celenza, J.L. and Carlson, M. 1984. Cloning and genetic mapping of SNF1, a gene required for expression of glucose-repressible genes in *Saccharomyces cerevisiae. Mol. Cell. Biol.* **4:** 49–53.

———. 1986. A yeast gene that is essential for release from glucose repression encodes a protein kinase. *Science* **233:** 1175–1180.

Chi, M.Y., Manchester, J., Yang, V., Curato, A., Strickler, R., and Lowry, O.H. 1988. Contrast in levels of metabolic enzymes in human and mouse ova. *Biol. Reprod.* **39:** 295–307.

Clark-Walker, G.D. and Azad, A.A. 1980. Hybridizable sequences between cytoplasmic ribosomal RNAs and 3 micron circular DNAs of *Saccharomyces cerevisiae* and *Torulopsis glabrata. Nucleic Acids Res.* **8:** 1009–1022.

DeRisi, J.L., Iyer, V.R., and Brown, P.O. 1997. Exploring the metabolic and genetic control of gene expression on a genomic scale. *Science* **78:** 680–686.

DeVit, M.J. and Johnston, M. 1999. The nuclear exportin Msn5 is required for nuclear export of the MIG 1 glucose repressor of *Saccharomyces cerevisiae. Curr. Biol.* **9:** 1231–1241.

DeVit, M.J., Waddle, J.A., and Johnston, M. 1997. Regulated nuclear translocation of the Mig1 glucose repressor. *Mol. Biol. Cell* **8:** 1603–1618.

Duronio, R.J., Towler, D.A., Heuckeroth, R.O., and Gordon, J.I. 1989. Disruption of the yeast *N*-myristoyltransferase gene causes recessive lethality. *Science* **243:** 796–800.

Ewbank, J.J., Barnes, T.M., Lakowski, B., Lussier, M., Bussey, H., and Hekimi, S. 1997. Structural and functional conversation of the *Caenorhabditis elegans* timing gene *clk-1. Science* **275:** 980–983.

Graves, J.L., Toolson, E.C., Jeong, C., Vu, L.N., and Rose, M.R. 1992. Desiccation, flight, glycogen and postponed senescence in *Drosophila melanogaster. Physiol. Zool.* **65:** 268–286.

Hardie, D.G., Carling, D., and Carlson, M. 1998. The AMP-activated/SNF1 protein kinase subfamily: Metabolic sensors of the eukaryotic cell? *Annu. Rev. Biochem.* **67:** 821–855.

Imai, S-I., Armstrong, C.M., Kaeberlein, M., and Guarente, L. 2000. Transcriptional silencing and longevity protein Sir2 is an NAD-dependent histone deacetylase. *Nature* **403:** 795–800.

Jiang, R. and Carlson, M. 1996. Glucose regulates protein interactions within the yeast *SNF1* protein kinase complex. *Genes & Dev.* **10:** 3105–3115.

———. 1997. The Snf1 protein kinase and its activating subunit, Snf4, interact with distinct domains of the Sip1/Sip2/Gal83 component in the kinase complex. *Mol. Cell. Biol.* **4:** 2099–2106.

Johnston, M. 1999. Feasting, fasting and fermenting glucose sensing in yeast and other cells. *Trends Genet.* **15:** 29–33.

Kennedy, B.K., Austriaco, N.R., Zhang, J., and Guarente, L. 1995. Mutation of silencing gene *SIR4* can delay aging in *S. cerevisiae. Cell* **80:** 485–496.

Kennedy, B.K., Gotta, M., Sinclair, D.A., Mills, K., McNabb, D.S., Murthy, M., Pak, S.M., Laroche, T., Gasser, S.M., and Guarente, L. 1997. Redistribution of silencing proteins from telomeres to the nucleolus is associated with extension of life span in *S. cerevisiae. Cell* **89:** 381–391.

Kenyon, C.J., Chang, J., Gensch, E., Rudner, A., and Tabtiang, R.A. 1993. A *C. elegans* mutant that lives twice as long as wild-type. *Nature* **366:** 461–464.

Kimura, K.D., Tissenbaum, H.A., Liu, Y., and Ruvkun, G. 1997. *daf-2,* an insulin receptor-like gene that regulates longevity and diapause in *Caenorhabditis elegans. Science* **277:** 942–946.

Klass, M.R. and Hirsch, D.I. 1976. Nonaging developmental variant of *C. elegans. Nature* **260:** 523–525.

Larionov, V.L., Grishin, A.V., and Smirnov, M.N. 1980. 3 micron DNA: An extrachromosomal ribosomal DNA in the yeast *Saccharomyces cerevisiae. Gene* **12:** 41–49.

Larionov, V.L., Kouprina, N., and Karpova, T. 1984. Stability of recombinant plasmids containing the *ARS* sequences of yeast extrachromosomal rDNA in several strains of *Saccharomyces cerevisiae. Gene* **28:** 229–235.

Larsen, P.L. 1993. Aging and resistance to oxidative damage in *Caenorhabditis elegans. Proc. Natl. Acad. Sci.* **90:** 8905–8909.

Lee, C.-K., Kloop, R.G., Weindruch, R., and Prolla, T.A. 1999. Gene expression profile of aging and its retardation by caloric restriction. *Science* **285:** 1390–1393.

Lin, K., Dorman, J., Rodan, A., and Kenyon, C.J. 1997. *daf-16*, a HNF-3/forkhead family member that can function to double the lifespan of *C. elegans. Science* **278:** 1319–1322.

Lin, Y.-J., Seroude, L., and Benzer, S. 1998. Extended life-span and stress resistance in the *Drosophila* mutant *methuselah. Science* **282:** 943–946.

Lithgow, G.J., White, T.M., Melov, S., and Johnson, T.E. 1995. Thermotolerance and extended life-span conferred by single-gene mutations and induced by thermal stress. *Proc. Natl. Acad. Sci.* **92:** 7540–7544.

Lowry, O.H. 1980. Amplification by emzymatic cycling. *Mol. Cell. Biol.* **32:** 135–146.

Ludin, K., Jiang, R., and Carlson, M. 1998. Glucose-regulated interaction of a regulatory subunit of protein phosphatase 1 with the Snf1 kinase in *Saccharomyces cerevisiae. Proc. Natl. Acad. Sci.* **95:** 6245–6250.

Manchester, J., Kong, X., Nerbonne, J., Lowry, O.H., and Lawrence, J.C. 1994. Glucose transport and phosphorylation in single cardiac myocytes: Rate limiting steps in glucose metabolism. *Am. J. Physiol.* **266:** E326–E333.

Mitchelhill, K.I., Stapleton, D., Gao, G., House, C., Michell, B., Katsis, F., Witters, L.A., and Kemp, B.E. 1994. Mammalian AMP-activated protein kinase shares structural and functional homology with the catalytic domain of yeast Snf1 protein kinase. *J. Biol. Chem.* **269:** 2361–2364.

Morris, J.Z., Tissenbaum, H.A., and Ruvkun, G. 1996. A phosphatidylinositol-3-OH kinase family member regulating longevity and diapause in *Caenorhabditis elegans. Nature* **382:** 536–539.

Mortimer, R.K. and Johnston, J.R. 1959. Life span of individual yeast cells. *Nature* **183:** 1751–1752.

Murakami, S. and Johnson, T.E. 1996. A genetic pathway conferring life extension and resistance to UV stress in *Caenorhabditis elegans. Genetics* **143:** 1207–1218.

Nehlin, J.O. and Ronne, H. 1990. Yeast *MIG1* repressor is related to the mammalian early growth response and Wilms' tumour finger proteins. *EMBO J.* **9:** 2891–2898.

Nehlin, J.O., Carlberg, M., and Ronne, H. 1991. Control of yeast *GAL* genes by *MIG1* repressor: A transcriptional cascade in the glucose response. *EMBO J.* **10:** 3373–3377.

Orr, W.C. and Sohal, R.S. 1994. Extension of life-span by overexpression of superoxide dismutase and catalase in *Drosophila melanogaster. Science* **263:** 1128–1130.

Passonneau, J.V. and Lowry, O.H. 1993. *Enzymatic analysis: A practical guide.* Humana Press, Totawa, NJ.

Service, P.M., Hutchinson, M., MacKinley, D., and Rose, M.R. 1985. Resistance to environmental stress in *Drosophila melanogaster* selected for postponed senescence. *Physiol. Zool.* **58:** 380–389.

Sinclair, D.A. and Guarente, L. 1997. Extrachromosomal rDNA circles: A cause of aging in yeast. *Cell* **91:** 1033–1042.

Sinclair, D.A., Mills, K., and Guarente, L. 1997. Accelerated aging and nucleolar fragmentation in yeast *sgs1* mutants. *Science* **277:** 1313–1316.

Smeal, T., Claus, J., Kennedy, B., Cole, F., and Guarente, L. 1996. Loss of transcriptional silencing causes sterility in old mother cells of *S. cerevisiae. Cell* **84:** 633–642.

Thompson-Jaeger, S., Francois, J., Gaughran, J.P., and Tatchell, K. 1991. Deletion of *SNF1* affects the nutrient response of

yeast and resembles mutations which activate the adenylate cyclase pathway. *Genetics* **129:** 697–706.
Vincent, O. and Carlson, M. 1999. Gal83 mediates the interaction of the Snf1 kinase complex with the transcription activator Sip4. *EMBO J.* **18:** 6672–6681.
Werner-Washburne, M., Braun, E., Johnston, G.C., and Singer, R.A. 1993. Stationary phase in the yeast *Saccharomyces cerevisiae. Micro. Rev.* **57:** 383–401.
Werner-Washburne, M., Braun, E.L., Crawford, M.E., and Peck, V.M. 1996. Stationary phase in *Saccharomyces cerevisiae. Mol. Microbiol.* **19:** 1159–1166.
Wood, W.B. 1998. Aging of *C. elegans*: Mosaics and mechanisms. *Cell* **95:** 147–150.
Yang, X., Jiang, R., and Carlson, M. 1994. A family of proteins containing a conserved domain that mediates interaction with the yeast *SNF1* protein kinase complex. *EMBO J.* **13:** 5878–5886.
Yu, C.-E., Oshima, J., Fu, Y.-H., Wijsman, E.M., Hisama, F., Alisch, R., Matthews, S., Nakura, J., Miki, T., Ouais, S., et al. 1996. Positional cloning of the Werner's syndrome gene. *Science* **272:** 258–262.